Table 2.1. Inflammation Associated with Aberrant DNA Methylation and Genes Methylated

Disease	Type of cancer induced	Methylated genes	Reference
HBV-asociated hepatitis	Liver cancer	*CDKN2A* (p16; P)	Narimatsu *et al.* (2004)
		CYP7B1 (P), *HOXA11* (P), *OCIAD2* (P), *RASGRF2* (P), *RRAD* (P), *RUNX3* (P), *SMOC2* (P), *TBX5* (P), *TUBB6* (P), *ZNF141* (P), *ZNF382* (P)	Deng *et al.* (in press)
HCV-associated hepatitis	Liver cancer	*CDKN2A* (p16; P)	Narimatsu *et al.* (2004)
		RUNX3 (P)	Nishida *et al.* (2008)
		CD38 (P), *CYP7B1* (P), *CYP24A1* (P), *JAKMIP1* (P), *NPR1* (P), *RRAD* (P), *RUNX3* (P), *TBX5* (P), *TUBB6* (P), *ZNF382* (P)	Deng *et al.* (in press)
Hemochromatosis	Liver cancer	*APC* (P), *CDKN2A* (p16; P), *CCND2* (P), *GSTP1* (P), *RASSF1A* (P), *SOCS1* (P)	Lehmann *et al.* (2007)
H.pylori-associated gastritis	Stomach cancer	*ARPC1B* (B), *CDKN2A* (p16; P, B), *FLNC* (P) *HAND1* (P), *HRASLS* (P) ,*LOX* (P), *THBD* (P)	Maekita *et al.* (2005)
		APC (P), *CDH1* (P), *CDKN2A* (p16; P), *COX2* (P), *MLH1* (P)	Perri *et al.* (2007)
Pancreatitis	Pancreatic cancer	*APC* (P), *BRCA1* (P), *CDKN2A* (p16; P), *CDKN2B* (P), *GSTP1*(P)	Peng *et al.* (2006)
Reflux esophagitis (Barret's esophagus)	Esophageal cancer	*CDKN2A* (p16; P)	Klump *et al.* (1998)
		APC (P), *CDKN2A* (p16; P), *ESR1* (P)	Eads *et al.* (2000)
		APC (P), *CDKN2A* (p16; P), *CRBP1* (P), *HPP1* (P), MGMT (P), *3-0ST-2* (P), *RIZ1* (P), *RUNX3* (P), *TIMP3* (P),	Schulmann *et al.* (2005)
		GPX3 (P), *GPX7* (P), *GSTM2* (P), GSTM3 (P)	Peng *et al.* (2008)
		APC (P), *CDKN2A* (p16; P)	Wang *et al.* (2009)
Ulcerative colitis	Colon cancer	*CDKN2A* (p16; P)	Hsieh *et al.* (1998)
		CDKN2A (p16; B), *ESR1* (B), *MYOD1* (P)	Issa *et al.* (2001)
		CDKN2A (p14; B)	Sato *et al.* (2002)

P, promoter region of the gene; B, gene body (exon and intron).

(p14 and p16) and *ESR1* (*ERα*)] (Issa *et al.*, 2001; Sato *et al.*, 2002). In addition, Barrett's esophagus frequently contains methylation of promoter CGIs of *CDKN2A* (p16), *HPP1*, and *RUNX3* (Eads *et al.*, 2000; Klump *et al.*, 1998; Schulmann *et al.*, 2005; Wang *et al.*, 2009). Livers with hepatitis due to infection of hepatitis viruses or hemochromatosis contain frequent methylation of promoter CGIs of *CDKN2A* (p16), *RASSF1A*, and *RUNX3* (Deng *et al.*, in press; Lehmann *et al.*, 2007; Narimatsu *et al.*, 2004; Nishida *et al.*, 2008).

In human gastric mucosae with inflammation due to *H. pylori* infection, aberrant methylation of multiple genes is present (Maekita *et al.*, 2006). Among the multiple CGIs methylated, the methylation level of a promoter CGI of a tumor-suppressor gene, *CDKN2A* (p16), was relatively low (<0.3%) compared to those of other nontumor suppressor genes such as *HAND1* and *THBD* (0.8–11.2%). The resistance of tumor-suppressor genes to DNA methylation induction is likely to be a general rule (Takeshima and Ushijima, 2010). The frequency of cells with aberrant methylation in gastric mucosae, which approximately equals the methylation level, is much higher than that of mutations induced by *H. pylori* infection, which is estimated to be one per 10^4–10^5 cells (Touati *et al.*, 2003). This suggests that induction of aberrant DNA methylation in gastric mucosae is an important carcinogenic mechanism by *H. pylori* infection.

2. Causal role of inflammation in induction of aberrant DNA methylation

The presence of aberrant DNA methylation in tissues with inflammation strongly indicates a causal role of inflammation in induction of aberrant DNA methylation. To experimentally demonstrate the causal role, we used an animal model of Mongolian gerbils in which *H. pylori* infection induces gastritis, aberrant DNA methylation of CGIs in gastric mucosal epithelial cells, and finally gastric cancers (Niwa *et al.*, 2010). Suppression of inflammation by an immunosuppressive reagent, cyclosporin A, did not affect colonization of *H. pylori*, but markedly repressed methylation induction by *H. pylori* infection. Therefore, although *H. pylori* infection is important to trigger inflammation capable of inducing aberrant DNA methylation, some inflammation processes appear to be critical in induction of aberrant DNA methylation.

3. Use of DNA methylation as a marker of past exposure to inflammation

Aberrant DNA methylation in tissue stem cells is expected to remain even after its inducing stimulus has disappeared. Indeed, *H. pylori* infection induces aberrant DNA methylation of specific CGIs, which will remain even after

eradication of *H. pylori* (Nakajima *et al.*, 2009; Niwa *et al.*, 2010). Smoking duration was shown to be correlated with methylation levels of specific genes in esophageal mucosae, where smoking is a risk factor of esophageal cancers (Oka *et al.*, 2009). These data suggest that some of the epigenetic alterations induced by inflammation remain and accumulate in noncancerous tissues, and that the accumulated alterations may serve as a marker of past exposure to inflammation.

B. DNA hypomethylation induced by inflammation

Global DNA hypomethylation, defined as a decrease in the content of 5-methylcytosine in the genome, is a hallmark of cancers (Feinberg *et al.*, 2006), and is often associated with hypomethylation of normally methylated repetitive sequences, such as LINE1, *Alu*, and Satα (Rollins *et al.*, 2006). Global hypomethylation has been shown to be involved in chromosomal instability and cancer development (Gaudet *et al.*, 2003; Holm *et al.*, 2005). In connection with inflammation, chronic inflammation is known to induce global DNA hypomethylation. In colonic mucosae of patients with UC, a marked decrease in the 5-methylcytosine content in the genome is present (Gloria *et al.*, 1996). In gastric mucosae of individuals infected with *H. pylori*, significant decreases in the methylation levels of *Alu* and Satα, but not LINE1, are present, whereas global hypomethylation is present only in some individuals (Yoshida *et al.*, in press).

C. Histone modification alterations induced by inflammation

Since aberrant DNA methylation is frequently observed in tissues with inflammation, histone modification alterations are expected to be present. However, so far, there is a very limited number of studies that assessed histone modification alterations in epithelial cells exposed to inflammation. Hahn *et al.* (2008) showed alteration of trimethylation of histone H3 at lysine 27 (H3K27me3) in mice exposed to ileocolitis due to genetic deficiency of *Gpx1* and *Gpx2*. One of the reasons why few reports are available in this field is the technical difficulty in analyzing histone modifications by chromatin immunoprecipitation. It requires complete separation of individual cells, which itself is difficult in tissue samples and can require time-consuming, and thus sample-degrading, steps.

D. An epigenetic field for cancerization

Aberrant DNA methylation and hypomethylation are present in noncancerous tissues that are undergoing or underwent inflammation, and methylation levels of specific genes correlate with risk of cancer development (Nakajima *et al.*, 2006a; Kaise *et al.*, 2008; Ushijima, 2007), as above discussed. Genes methylated in noncancerous tissues involve both tumor-suppressor genes, such as *CDKN2A*,

and other passenger genes, such as *FLNc* and *THBD* (Maekita *et al.*, 2006). The condition that a significant number of cells in a tissue has already accumulated aberrant methylation of tumor-suppressor genes (and passenger genes) has a high risk of developing cancers is referred to as "an epigenetic field for cancerization" or "an epigenetic field defect."

For cancer prevention, the presence of an epigenetic field defect indicates that inhibition of induction of epigenetic alterations is likely to be effective, and that the effectiveness of a method can be assessed by measuring the degree of epigenetic field defects. It also suggests that removal of accumulated epigenetic alterations might be effective for prevention of cancer development, although we need to be cautious not to remove physiologically necessary DNA methylation or any other epigenetic modifications.

IV. MECHANISMS FOR INDUCTION OF EPIGENETIC ALTERATIONS BY INFLAMMATION

Mechanisms for induction of epigenetic alterations by inflammation are still unclear. Inflammation is characterized by disturbance of cytokine signals and induction of cell proliferation, but it is still unclear how these abnormalities lead to induction of aberrant DNA methylation. Although it had been unclear whether there is gene specificity in methylation induction by inflammation, the presence of specificity and its mechanisms are becoming clear.

A. Disturbance of cytokine signals

In tissues with inflammation, many inflammatory cytokines and chemokines are produced by inflammatory cells and epithelial cells, depending on the types of inflammation. These cytokines and chemokines are essential for inflammation, and they are likely to be involved in induction of epigenetic alterations. In gerbil gastric mucosae infected with *H. pylori*, expression of *Cxcl2* (a functional homolog of human *IL8*), *Il1b*, *Nos2*, and *Tnf* is associated with induction of DNA methylation (Niwa *et al.*, 2010). Three of these four factors are also upregulated in human hepatitis and UC (Cappello *et al.*, 1992; Llorente *et al.*, 1996; McLaughlan *et al.*, 1997). Especially for *IL1B*, its promoter polymorphism responsible for overproduction of IL1B protein is associated with risk of human gastric cancers and with methylation of multiple genes in gastric cancers (Chan *et al.*, 2007; El-Omar *et al.*, 2000). However, so far, it is unclear how individual cytokines and chemokines change the molecular machinery of DNA methylation in epithelial cells exposed to them.

B. Induction of cell proliferation

Inflammation induces proliferation of epithelial cells to compensate loss of damaged cells and repair tissue organization. It is well known that aberrant DNA methylation of some genes is induced by aging (Issa *et al.*, 1994). Therefore, one of the important mechanisms of how inflammation induces aberrant DNA methylation is acceleration of cell proliferation (Issa *et al.*, 2001). By analysis of *Gpx1/Gpx2* KO mice, some genes that undergo age-dependent DNA methylation were shown to have increased levels of DNA methylation, and induction of cell proliferation was indicated as an accelerator of age-dependent DNA methylation. However, notably, the majority (~70%) of genes that undergo age-dependent methylation were not methylated by inflammation (Hahn *et al.*, 2008), and methylation induced by inflammation was suggested to have different target genes from aging.

C. Mechanisms for gene specificity in induction of aberrant DNA methylation

There is clear gene specificity in induction of aberrant DNA methylation according to tissue types and inducers (Costello *et al.*, 2000; Nakajima *et al.*, 2009; Oka *et al.*, 2009). As determinants of the susceptibility, gene expression, the presence of RNA polymerase II (Pol II) (active or stalled), and the presence of specific histone modifications, such as trimethylation of lysine 27 of histone H3 (H3K27me3), are known (Takeshima and Ushijima, 2010; Takeshima *et al.*, 2009).

Genes with low gene expression are susceptible to induction of DNA methylation in cell lines (De Smet *et al.*, 2004; Song *et al.*, 2002) and in human tissues (Nakajima *et al.*, 2009). Susceptibility was also observed in a genome-wide analysis (Takeshima *et al.*, 2009). Genes with H3K27me3 in embryonic stem cells and/or normal epithelial cells were shown to tend to be methylated in cancers for specific genes (Ohm *et al.*, 2007; Schlesinger *et al.*, 2007; Widschwendter *et al.*, 2007), and the association was also confirmed in a genome-wide study (Gal-Yam *et al.*, 2008). On the other hand, the presence of Pol II, active or stalled, is associated with resistance to induction of DNA methylation (Genes A and B in Fig. 2.2; Takeshima *et al.*, 2009).

It can be speculated that inflammation induces decreased expression of some genes (Gene C) and eliminates stalled Pol II (Genes C and D), and recruits a polycomb complex to induce H3K27me3. This could lead to DNA methylation of genes that are not susceptible without inflammation. Genes that physiologically have H3K27me3 can also be methylated by inflammation (Gene E). For example, in ileocolitis of *Gpx1/Gpx2* mice, aberrant DNA methylation was

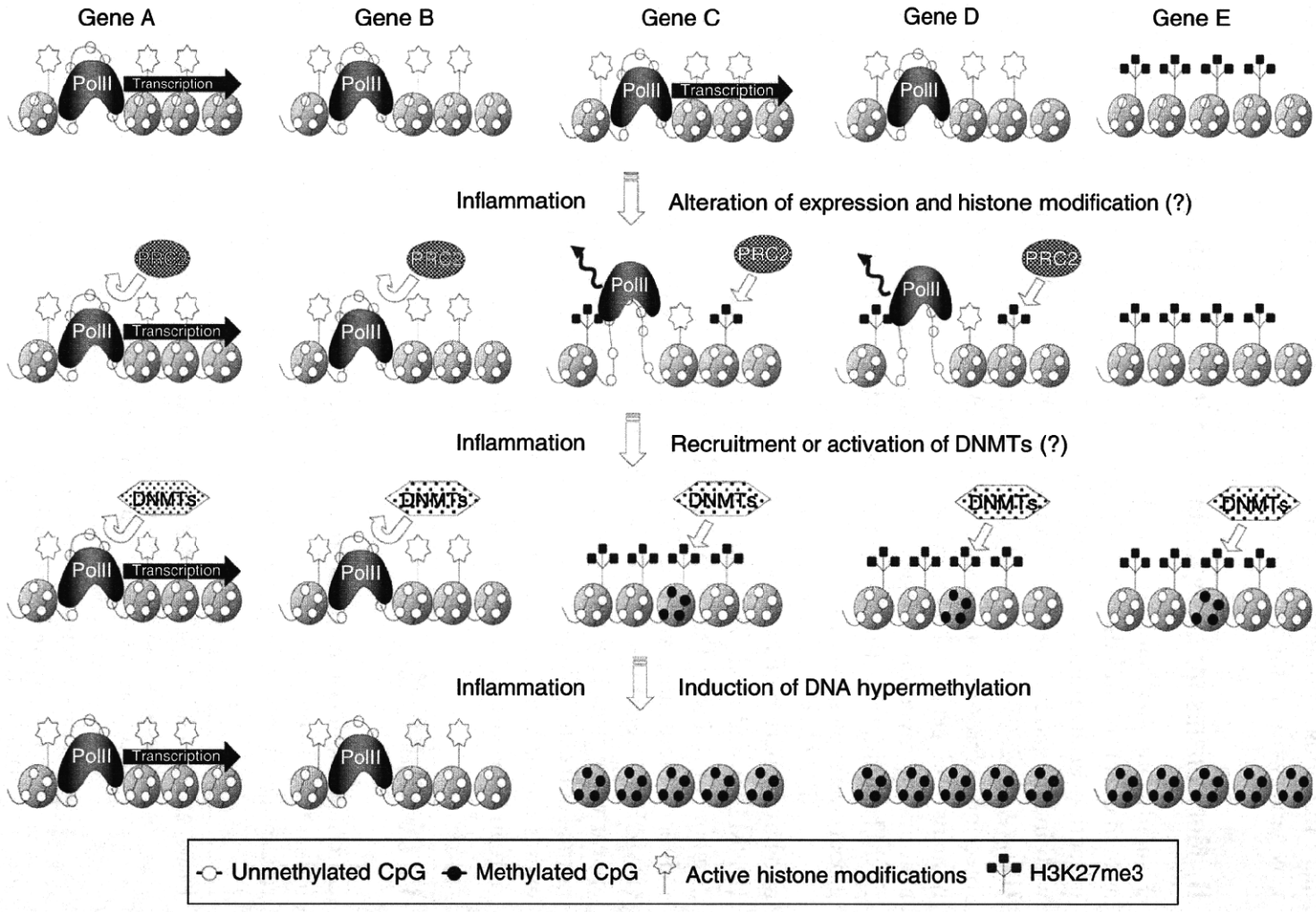

Figure 2.2. (Continued)

induced in epithelial cells, and 59% of the methylated genes had an H3K27me3 mark in normal epithelial cells (Hahn *et al.*, 2008). However, it is still unclear why genes without the H3K27me3 mark were also methylated.

D. Mechanisms for methylation induction at specific genes

To methylate DNA molecules, DNA methyltransferases (DNMTs) are essential as final effectors, and their overexpression has been suggested to be involved in induction of aberrant DNA methylation. Indeed, in the liver and pancreases with inflammation, overexpression of DNMT1 mRNA or protein was observed (Peng *et al.*, 2005; Sun *et al.*, 1997). In contrast, in gastric mucosae with *H. pylori* infection, expression of *DNMT1*, *DNMT3A*, and *DNMT3B* is not increased in humans and gerbils (Nakajima *et al.*, 2009; Niwa *et al.*, 2010). Therefore, aberrant methylation is likely to be induced by a local imbalance between DNMTs and factors that protect genes from DNA methylation, in addition to global overexpression of DNMTs.

EZH2, which is a component of polycomb repressive complex 2 (PRC2) and has a function of a methylase of H3K27, is reported to interact with DNMTs (DNMT3A and DNMT3B) directly (Vire *et al.*, 2006). In addition, BMI1 is a component of PRC1 that recognizes H3K27me3 marks, and was shown to have indirect interaction with DNMT1 through DNMT1-associated protein 1 (DMAP1) (Negishi *et al.*, 2007). These factors (EZH2, BMI1, and DMAP1) appear to be necessary for the maintenance of some CGI methylation in both normal and cancer cells (Negishi *et al.*, 2007; Vire *et al.*, 2006). Thus, changes in expression or localization of these factors by inflammation may link inflammation and aberrant methylation induction (Fig2.2, gene C and D).

V. CONCLUSIONS

Chronic inflammation appears to induce aberrant epigenetic alterations, and the induction is likely to be one of the major mechanisms of how chronic inflammation induces cancers. However, the molecular mechanisms underlying induction

Figure 2.2. Scheme of aberrant DNA methylation induction by inflammation. Genes with H3K27me3, which have little expression, have high risk of being methylated by inflammation (Genes E), and recruitment of DNMTs to the H3K27me3 mark is likely to be one of its mechanisms. In contrast, genes with active histone modification and Pol II are resistant to methylation induction, regardless of their expression levels (Genes A and B). Active histone marks and Pol II localization might prevent recruitment of DNMTs. If localization of active histone modification and Pol II is disturbed by inflammation, it leads to recruitment of PRC2 and DNMTs, which can result in de novo methylation (Genes C and D).

of aberrant DNA methylation are largely unknown. Research focusing on individual cytokines and chemokines and local balance between DNMTs and protecting factors, such as the presence of Pol II, along with histone modification alterations induced by inflammation, are expected to offer clues to uncover the mechanisms.

Acknowledgment

This study was supported by Grants-in-Aid for Cancer Research from the Ministry of Health, Labour and Welfare, Japan.

References

Bianchi, C., and Bianchi, T. (2007). Malignant mesothelioma: Global incidence and relationship with asbestos. *Ind. Health* **45,** 379–387.

Cappello, M., Keshav, S., Prince, C., Jewell, D. P., and Gordon, S. (1992). Detection of mRNAs for macrophage products in inflammatory bowel disease by in situ hybridisation. *Gut* **33,** 1214–1219.

Castellone, M. D., Teramoto, H., Williams, B. O., Druey, K. M., and Gutkind, J. S. (2005). Prostaglandin E2 promotes colon cancer cell growth through a Gs-axin-beta-catenin signaling axis. *Science* **310,** 1504–1510.

Chan, A. O., Chu, K. M., Huang, C., Lam, K. F., Leung, S. Y., Sun, Y. W., Ko, S., Xia, H. H., Cho, C. H., Hui, W. M., *et al.* (2007). Association between Helicobacter pylori infection and interleukin 1beta polymorphism predispose to CpG island methylation in gastric cancer. *Gut* **56,** 595–597.

Choi, P. M., and Zelig, M. P. (1994). Similarity of colorectal cancer in Crohn's disease and ulcerative colitis: Implications for carcinogenesis and prevention. *Gut* **35,** 950–954.

Costello, J. F., Fruhwald, M. C., Smiraglia, D. J., Rush, L. J., Robertson, G. P., Gao, X., Wright, F. A., Feramisco, J. D., Peltomaki, P., Lang, J. C., *et al.* (2000). Aberrant CpG-island methylation has non-random and tumour-type-specific patterns. *Nat. Genet.* **24,** 132–138.

Cotran, R. S., Kumar, V., and Robbins, S. L. (1989). Robbins pathologic basis of disease W.B. Saunders company, Philadelphia.

De Smet, C., Loriot, A., and Boon, T. (2004). Promoter-dependent mechanism leading to selective hypomethylation within the 5′ region of gene MAGE-A1 in tumor cells. *Mol. Cell. Biol.* **24,** 4781–4790.

Deng, Y. B., Nagae, G., Midorikawa, Y., Yagi, K., Tsutsumi, S., Yamamoto, S., Hasegawa, K., Kokudo, N., Aburatani, H., and Kaneda, A. (2010). Identification of genes preferentially methylated in hepatitis C virus-related hepatocellular carcinoma. *Cancer Sci.* (in press).

Eads, C. A., Lord, R. V., Kurumboor, S. K., Wickramasinghe, K., Skinner, M. L., Long, T. I., Peters, J. H., DeMeester, T. R., Danenberg, K. D., Danenberg, P. V., *et al.* (2000). Fields of aberrant CpG island hypermethylation in Barrett's esophagus and associated adenocarcinoma. *Cancer Res.* **60,** 5021–5026.

Ekbom, A., Helmick, C., Zack, M., and Adami, H. O. (1990a). Increased risk of large-bowel cancer in Crohn's disease with colonic involvement. *Lancet* **336,** 357–359.

Ekbom, A., Helmick, C., Zack, M., and Adami, H. O. (1990b). Ulcerative colitis and colorectal cancer: A population-based study. *N. Engl. J. Med.* **323,** 1228–1233.

Ekstrom, A. M., Held, M., Hansson, L. E., Engstrand, L., and Nyren, O. (2001). Helicobacter pylori in gastric cancer established by CagA immunoblot as a marker of past infection. *Gastroenterology* **121,** 784–791.

El-Omar, E. M., Carrington, M., Chow, W. H., McColl, K. E., Bream, J. H., Young, H. A., Herrera, J., Lissowska, J., Yuan, C. C., Rothman, N., *et al.* (2000). Interleukin-1 polymorphisms associated with increased risk of gastric cancer. *Nature* **404,** 398–402.

Federico, A., Morgillo, F., Tuccillo, C., Ciardiello, F., and Loguercio, C. (2007). Chronic inflammation and oxidative stress in human carcinogenesis. *Int. J. Cancer* **121,** 2381–2386.

Feinberg, A. P., Ohlsson, R., and Henikoff, S. (2006). The epigenetic progenitor origin of human cancer. *Nat. Rev. Genet.* **7,** 21–33.

Gal-Yam, E. N., Egger, G., Iniguez, L., Holster, H., Einarsson, S., Zhang, X., Lin, J. C., Liang, G., Jones, P. A., and Tanay, A. (2008). Frequent switching of Polycomb repressive marks and DNA hypermethylation in the PC3 prostate cancer cell line. *Proc. Natl. Acad. Sci. USA* **105,** 12979–12984.

Gaudet, F., Hodgson, J. G., Eden, A., Jackson-Grusby, L., Dausman, J., Gray, J. W., Leonhardt, H., and Jaenisch, R. (2003). Induction of tumors in mice by genomic hypomethylation. *Science* **300,** 489–492.

Gloria, L., Cravo, M., Pinto, A., de Sousa, L. S., Chaves, P., Leitao, C. N., Quina, M., Mira, F. C., and Soares, J. (1996). DNA hypomethylation and proliferative activity are increased in the rectal mucosa of patients with long-standing ulcerative colitis. *Cancer* **78,** 2300–2306.

Gomaa, A. I., Khan, S. A., Toledano, M. B., Waked, I., and Taylor-Robinson, S. D. (2008). Hepatocellular carcinoma: epidemiology, risk factors and pathogenesis. *World J. Gastroenterol.* **14,** 4300–4308.

Hahn, M. A., Hahn, T., Lee, D. H., Esworthy, R. S., Kim, B. W., Riggs, A. D., Chu, F. F., and Pfeifer, G. P. (2008). Methylation of polycomb target genes in intestinal cancer is mediated by inflammation. *Cancer Res.* **68,** 10280–10289.

Heintz, N. H., Janssen, Y. M., and Mossman, B. T. (1993). Persistent induction of c-fos and c-jun expression by asbestos. *Proc. Natl. Acad. Sci. USA* **90,** 3299–3303.

Holm, T. M., Jackson-Grusby, L., Brambrink, T., Yamada, Y., Rideout, W. M., 3rd., and Jaenisch, R. (2005). Global loss of imprinting leads to widespread tumorigenesis in adult mice. *Cancer Cell* **8,** 275–285.

Hsieh, C. J., Klump, B., Holzmann, K., Borchard, F., Gregor, M., and Porschen, R. (1998). Hypermethylation of the p16INK4a promoter in colectomy specimens of patients with long-standing and extensive ulcerative colitis. *Cancer Res.* **58,** 3942–3945.

Hussain, S. P., and Harris, C. C. (2007). Inflammation and cancer: An ancient link with novel potentials. *Int. J. Cancer* **121,** 2373–2380.

Issa, J. P., Ahuja, N., Toyota, M., Bronner, M. P., and Brentnall, T. A. (2001). Accelerated age-related CpG island methylation in ulcerative colitis. *Cancer Res.* **61,** 3573–3577.

Issa, J. P., Ottaviano, Y. L., Celano, P., Hamilton, S. R., Davidson, N. E., and Baylin, S. B. (1994). Methylation of the oestrogen receptor CpG island links ageing and neoplasia in human colon. *Nat. Genet.* **7,** 536–540.

Kaise, M., Yamasaki, T., Yonezawa, J., Miwa, J., Ohta, Y., and Tajiri, H. (2008). CpG island hypermethylation of tumor-suppressor genes in H. pylori-infected non-neoplastic gastric mucosa is linked with gastric cancer risk. *Helicobacter* **13,** 35–41.

Kim, S. F., Huri, D. A., and Snyder, S. H. (2005). Inducible nitric oxide synthase binds, S-nitrosylates, and activates cyclooxygenase-2. *Science* **310,** 1966–1970.

Klump, B., Hsieh, C. J., Holzmann, K., Gregor, M., and Porschen, R. (1998). Hypermethylation of the CDKN2/p16 promoter during neoplastic progression in Barrett's esophagus. *Gastroenterology* **115,** 1381–1386.

Lehmann, U., Wingen, L. U., Brakensiek, K., Wedemeyer, H., Becker, T., Heim, A., Metzig, K., Hasemeier, B., Kreipe, H., and Flemming, P. (2007). Epigenetic defects of hepatocellular carcinoma are already found in non-neoplastic liver cells from patients with hereditary haemochromatosis. *Hum. Mol. Genet.* **16,** 1335–1342.

Llorente, L., Richaud-Patin, Y., Alcocer-Castillejos, N., Ruiz-Soto, R., Mercado, M. A., Orozco, H., Gamboa-Dominguez, A., and Alcocer-Varela, J. (1996). Cytokine gene expression in cirrhotic and non-cirrhotic human liver. *J. Hepatol.* **24,** 555–563.

Maekita, T., Nakazawa, K., Mihara, M., Nakajima, T., Yanaoka, K., Iguchi, M., Arii, K., Kaneda, A., Tsukamoto, T., Tatematsu, M., *et al.* (2006). High levels of aberrant DNA methylation in Helicobacter pylori-infected gastric mucosae and its possible association with gastric cancer risk. *Clin. Cancer Res.* **12,** 989–995.

McLaughlan, J. M., Seth, R., Vautier, G., Robins, R. A., Scott, B. B., Hawkey, C. J., and Jenkins, D. (1997). Interleukin-8 and inducible nitric oxide synthase mRNA levels in inflammatory bowel disease at first presentation. *J. Pathol.* **181,** 87–92.

Nakajima, T., Maekita, T., Oda, I., Gotoda, T., Yamamoto, S., Umemura, S., Ichinose, M., Sugimura, T., Ushijima, T., and Saito, D. (2006a). Higher methylation levels in gastric mucosae significantly correlate with higher risk of gastric cancers. *Cancer Epidemiol. Biomarkers Prev.* **15,** 2317–2321.

Nakajima, T., Oda, I., Gotoda, T., Hamanaka, H., Eguchi, T., Yokoi, C., and Saito, D. (2006b). Metachronous gastric cancers after endoscopic resection: How effective is annual endoscopic surveillance? *Gastric Cancer* **9,** 93–98.

Nakajima, T., Yamashita, S., Maekita, T., Niwa, T., Nakazawa, K., and Ushijima, T. (2009). The presence of a methylation fingerprint of Helicobacter pylori infection in human gastric mucosae. *Int. J. Cancer* **124,** 905–910.

Narimatsu, T., Tamori, A., Koh, N., Kubo, S., Hirohashi, K., Yano, Y., Arakawa, T., Otani, S., and Nishiguchi, S. (2004). p16 promoter hypermethylation in human hepatocellular carcinoma with or without hepatitis virus infection. *Intervirology* **47,** 26–31.

Negishi, M., Saraya, A., Miyagi, S., Nagao, K., Inagaki, Y., Nishikawa, M., Tajima, S., Koseki, H., Tsuda, H., Takasaki, Y., *et al.* (2007). Bmi1 cooperates with Dnmt1-associated protein 1 in gene silencing. *Biochem. Biophys. Res. Commun.* **353,** 992–998.

Nishida, N., Nagasaka, T., Nishimura, T., Ikai, I., Boland, C. R., and Goel, A. (2008). Aberrant methylation of multiple tumor suppressor genes in aging liver, chronic hepatitis, and hepatocellular carcinoma. *Hepatology* **47,** 908–918.

Niwa, T., Tsukamoto, T., Toyoda, T., Mori, A., Tanaka, H., Maekita, T., Ichinose, M., Tatematsu, M., and Ushijima, T. (2010). Inflammatory Processes Triggered by Helicobacter pylori Infection Cause Aberrant DNA Methylation in Gastric Epithelial Cells. *Cancer Res.* **70,** 1430–1440.

Ohm, J. E., McGarvey, K. M., Yu, X., Cheng, L., Schuebel, K. E., Cope, L., Mohammad, H. P., Chen, W., Daniel, V. C., Yu, W., *et al.* (2007). A stem cell-like chromatin pattern may predispose tumor suppressor genes to DNA hypermethylation and heritable silencing. *Nat. Genet.* **39,** 237–242.

Oka, D., Yamashita, S., Tomioka, T., Nakanishi, Y., Kato, H., Kaminishi, M., and Ushijima, T. (2009). The presence of aberrant DNA methylation in noncancerous esophageal mucosae in association with smoking history: A target for risk diagnosis and prevention of esophageal cancers. *Cancer* **115,** 3412–3426.

Peng, D. F., Kanai, Y., Sawada, M., Ushijima, S., Hiraoka, N., Kosuge, T., and Hirohashi, S. (2005). Increased DNA methyltransferase 1 (DNMT1) protein expression in precancerous conditions and ductal carcinomas of the pancreas. *Cancer Sci.* **96,** 403–408.

Rollins, R. A., Haghighi, F., Edwards, J. R., Das, R., Zhang, M. Q., Ju, J., and Bestor, T. H. (2006). Large-scale structure of genomic methylation patterns. *Genome Res.* **16,** 157–163.

Saadat, I., Higashi, H., Obuse, C., Umeda, M., Murata-Kamiya, N., Saito, Y., Lu, H., Ohnishi, N., Azuma, T., Suzuki, A., *et al.* (2007). Helicobacter pylori CagA targets PAR1/MARK kinase to disrupt epithelial cell polarity. *Nature* **447,** 330–333.

Sato, F., Harpaz, N., Shibata, D., Xu, Y., Yin, J., Mori, Y., Zou, T. T., Wang, S., Desai, K., Leytin, A., *et al.* (2002). Hypermethylation of the p14(ARF) gene in ulcerative colitis-associated colorectal carcinogenesis. *Cancer Res.* **62,** 1148–1151.

Schlesinger, Y., Straussman, R., Keshet, I., Farkash, S., Hecht, M., Zimmerman, J., Eden, E., Yakhini, Z., Ben-Shushan, E., Reubinoff, B. E., *et al.* (2007). Polycomb-mediated methylation on Lys27 of histone H3 pre-marks genes for de novo methylation in cancer. *Nat. Genet.* **39,** 232–236.

Schulmann, K., Sterian, A., Berki, A., Yin, J., Sato, F., Xu, Y., Olaru, A., Wang, S., Mori, Y., Deacu, E., *et al.* (2005). Inactivation of p16, RUNX3, and HPP1 occurs early in Barrett's-associated neoplastic progression and predicts progression risk. *Oncogene* **24,** 4138–4148.

Shin, H. R., Oh, J. K., Masuyer, E., Curado, M. P., Bouvard, V., Fang, Y. Y., Wiangnon, S., Sripa, B., and Hong, S. T. (2010). Epidemiology of cholangiocarcinoma: An update focusing on risk factors. *Cancer Sci.* **101,** 579–585.

Solaymani-Dodaran, M., Logan, R. F., West, J., Card, T., and Coupland, C. (2004). Risk of oesophageal cancer in Barrett's oesophagus and gastro-oesophageal reflux. *Gut* **53,** 1070–1074.

Song, J. Z., Stirzaker, C., Harrison, J., Melki, J. R., and Clark, S. J. (2002). Hypermethylation trigger of the glutathione-S-transferase gene (GSTP1) in prostate cancer cells. *Oncogene* **21,** 1048–1061.

Sun, L., Hui, A. M., Kanai, Y., Sakamoto, M., and Hirohashi, S. (1997). Increased DNA methyltransferase expression is associated with an early stage of human hepatocarcinogenesis. *Jpn. J. Cancer Res.* **88,** 1165–1170.

Takeshima, H., and Ushijima, T. (2010). Methylation destiny: Moira takes account of histones and RNA polymerase II. *Epigenetics* **5,** 89–95.

Takeshima, H., Yamashita, S., Shimazu, T., Niwa, T., and Ushijima, T. (2009). The presence of RNA polymerase II, active or stalled, predicts epigenetic fate of promoter CpG islands. *Genome Res.* **19,** 1974–1982.

Tomatis, L. (1993). Cell proliferation and carcinogenesis: A brief history and current view based on an IARC workshop report. International Agency for Research on Cancer. *Environ. Health Perspect.* **101**(Suppl 5), 149–151.

Touati, E., Michel, V., Thiberge, J. M., Wuscher, N., Huerre, M., and Labigne, A. (2003). Chronic Helicobacter pylori infections induce gastric mutations in mice. *Gastroenterology* **124,** 1408–1419.

Ushijima, T. (2007). Epigenetic field for cancerization. *J. Biochem. Mol. Biol.* **40,** 142–150.

Vire, E., Brenner, C., Deplus, R., Blanchon, L., Fraga, M., Didelot, C., Morey, L., Van Eynde, A., Bernard, D., Vanderwinden, J. M., *et al.* (2006). The Polycomb group protein EZH2 directly controls DNA methylation. *Nature* **439,** 871–874.

Wang, J. S., Guo, M., Montgomery, E. A., Thompson, R. E., Cosby, H., Hicks, L., Wang, S., Herman, J. G., and Canto, M. I. (2009). DNA promoter hypermethylation of p16 and APC predicts neoplastic progression in Barrett's esophagus. *Am. J. Gastroenterol.* **104,** 2153–2160.

Widschwendter, M., Fiegl, H., Egle, D., Mueller-Holzner, E., Spizzo, G., Marth, C., Weisenberger, D. J., Campan, M., Young, J., Jacobs, I., *et al.* (2007). Epigenetic stem cell signature in cancer. *Nat. Genet.* **39,** 157–158.

Yamashita, S., Hosoya, K., Gyobu, K., Takeshima, H., and Ushijima, T. (2009). Development of a novel output value for quantitative assessment in methylated DNA immunoprecipitation-CpG island microarray analysis. *DNA Res.* **16,** 275–286.

Yoshida, T., Yamashita, S., Takamura-Enya, T., Niwa, T., Ando, T., Enomoto, S., Maekita, T., Nakazawa, K., Tatematsu, M., Ichinose, M., et al. Alu and Satalpha hypomethylation in Helicobacter pylori-infected gastric mucosae. Int J Cancer. (in press)

Addiction Biology

PRECLINICAL STUDY: BRIEF REPORT

doi:10.1111/j.1369-1600.2010.00219.x

Epigenetic modulation at the CCR2 gene correlates with the maintenance of behavioral sensitization to methamphetamine

Daigo Ikegami[1], Minoru Narita[1], Satoshi Imai[1], Kazuhiko Miyashita[1], Rie Tamura[1], Michiko Narita[1], Shigemi Takagi[1], Akiko Yokomizo[1], Hideyuki Takeshima[2], Takayuki Ando[2], Katsuhide Igarashi[3], Jun Kanno[3], Naoko Kuzumaki[1], Toshikazu Ushijima[2] & Tsutomu Suzuki[1]

Department of Toxicology, Hoshi University School of Pharmacy and Pharmaceutical Sciences, Japan[1], Carcinogenesis Division, National Cancer Center Research Institute, Japan[2] and Division of Cellular & Molecular Toxicology, Biological Safety Research Center, National Institute of Health Sciences, Japan[3]

ABSTRACT

The intermittent administration of methamphetamine produces behavioral sensitization to methamphetamine. In the limbic forebrain, mainly including the nucleus accumbens, of mice that had been intermittently treated with methamphetamine, we found a significant increase in mRNA of a chemokine, CCR2. This increase was accompanied by a significant increase in histone H3 lysine 4 (H3K4) trimethylation at its promoter. Interestingly, the maintenance of sensitization to methamphetamine-induced hyperlocomotion was significantly decreased in CCR2 knockout mice. These findings suggest that increased CCR2 associated with epigenetic modification after the intermittent administration of methamphetamine may be associated with the maintenance of sensitization to methamphetamine-induced hyperlocomotion.

Keywords CCR2, drug abuse, epigenetics, histone modification, methamphetamine, sensitization.

Correspondence to: Minoru Narita and Tsutomu Suzuki, Department of Toxicology, Hoshi University School of Pharmacy and Pharmaceutical Sciences, 2-4-41 Ebara, Shinagawa-ku, Tokyo 142-8501, Japan. E-mail: narita@hoshi.ac.jp and suzuki@hoshi.ac.jp

Methamphetamine is a strongly addictive psychostimulant that dramatically affects the central nervous system (CNS) and is highly abused worldwide. In rodents, it has been shown consistently that repeated exposure to psychostimulants results in a progressive and enduring enhancement of the motor stimulant effect elicited by a subsequent drug challenge, which is called behavioral sensitization. Many studies have suggested that the mesolimbic dopaminergic system, which projects from the ventral tegmental area to the nucleus accumbens, is critical for the initiation of methamphetamine-induced hyperlocomotion (Vanderschuren & Kalivas 2000).

A growing body of evidence suggests that the behavioral sensitization induced by psychostimulants may be accompanied by long-lasting neural plasticity (Robinson & Kolb 1999). The neuronal plasticity has been believed to require diverse alterations in gene expression. Although some of the candidate genes that are involved in behavioral sensitization to psychostimulants have been identified (Ujike *et al.* 2002; Sokolov, Polesskaya & Uhl 2003), an important step toward unraveling the complex machinery of psychostimulant-induced behavioral sensitization is a multiplex analysis for both gene expression profiling and epigenetic modifications, which exert lasting control over gene expression without altering the genetic code.

Recent evidence has suggested that epigenetic mechanisms contribute to drug-induced transcriptional and behavioral changes (Renthal & Nestler 2008). Such epigenetic modulation is mainly controlled by histone modification. Histones are modified at many sites. Previously published reports have indicated that the increased acetylation of histone H3 or methylation of H3 at K4 (lysine 4) highly predicts gene activation, while increased methylation of H3 at K9 or K27 (lysine 9 or 27) is predictives of gene repression. The triggering of signaling cascades in target neurons leads to more long-lasting effects, including changes in gene expression via the control of transcription and thereby, chromatin remodeling.

In the present study, we report for the first time that the intermittent administration of methamphetamine increases the mRNA level of a C-C chemokine, CCR2, with histone modification in the limbic forebrain including the nucleus accumbens. To address the functional relevance of this increased CCR2 expression, we also investigated whether the increased locomotion observed after the intermittent administration of methamphetamine could be affected in CCR2 knockout mice.

The locomotor activity of mice was measured by an ambulometer (ANB-M20, O'Hara, Tokyo, Japan) as described previously. Briefly, male C57BL/6J mice or CCR2 knockout mice were obtained from Jackson Laboratories (Bar Harbor, ME, USA) and individually placed in a tilting-type round activity cage. To induce behavioral sensitization to methamphetamine-induced hyperlocomotion, the mice were given five intermittent treatments with methamphetamine (2 mg/kg, s.c.), once every 96 hours. To clarify the maintenance of behavioral sensitization, the mice were again administered methamphetamine (2 mg/kg, s.c.) after seven weeks of withdrawal.

The limbic forebrain area, mainly including the nucleus accumbens, was removed 24 hours after the last injection of methamphetamine. RNA preparation and semiquantitative analysis by reverse transcription polymerase chain reaction (RT-PCR) were performed as described previously. The methods are described in detail in the Supporting Information. The primers used are listed in Table S1.

Chromatin immunoprecipitation (ChIP) was performed as described previously with minor modifications. Soluble chromatin extracted from the mouse limbic forebrain was incubated with specific antibodies against acetylated histone H3 (Millipore; Billerica, MA, USA), H3K4 trimethylation (Wako Pure Chemicals, Osaka, Japan), H3K9 trimethylation (Millipore) and H3K27 trimethylation (Millipore) overnight at 4°C. The immunocomplex was collected by Dynabeads Protein A (Invitrogen Dynal AS, Oslo, Norway), and DNA was recovered by isopropanol precipitation. The methods are described in detail in the Supporting Information. The statistical analysis is also described in detail in the Supporting Information.

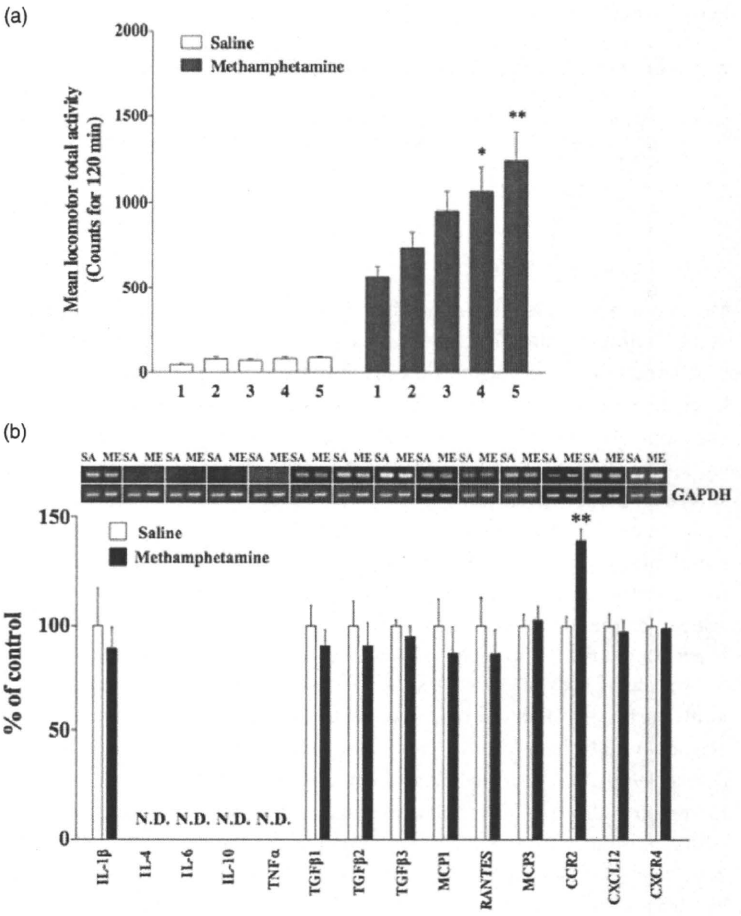

Figure 1 (a) Development of sensitization to methamphetamine in mice. Methamphetamine (2 mg/kg, s.c.) or saline was repeatedly given five times to mice every 96 hours. Total activity was counted for 120 minutes after each injection. Each column represents the mean total counts for 120 minutes with S.E.M. of 20 mice. (*$P < 0.01$, **$P < 0.001$ versus METH 1st). (b) Upper: Representative RT-PCR with 35 cycles for IL1β, IL-4, IL-6, IL-10, TNFα, TGFβ1, TGFβ2, TGFβ3, MCP1, RANTES, MCP3, CCR2, CXCL12 and CXCR4 mRNAs in the limbic forebrain of mice that have shown behavioral sensitization to methamphetamine (ME). The limbic forebrain sample was prepared 24 hours after the last injection of saline (SA) or ME. Lower: The intensity of the aforementioned bands was semi-quantified using Image J software. The value for mRNA was normalized by that for the internal standard glyceraldehyde-3-phosphate dehydrogenase (GAPDH) mRNA. The value for mice treated with methamphetamine is expressed as a percentage of the increase in mice treated with saline. Each column represents the mean ± SEM ($n = 3$ animals per group; three independent experiments). N.D., not detectable. **$P < 0.01$ versus saline-treated mice

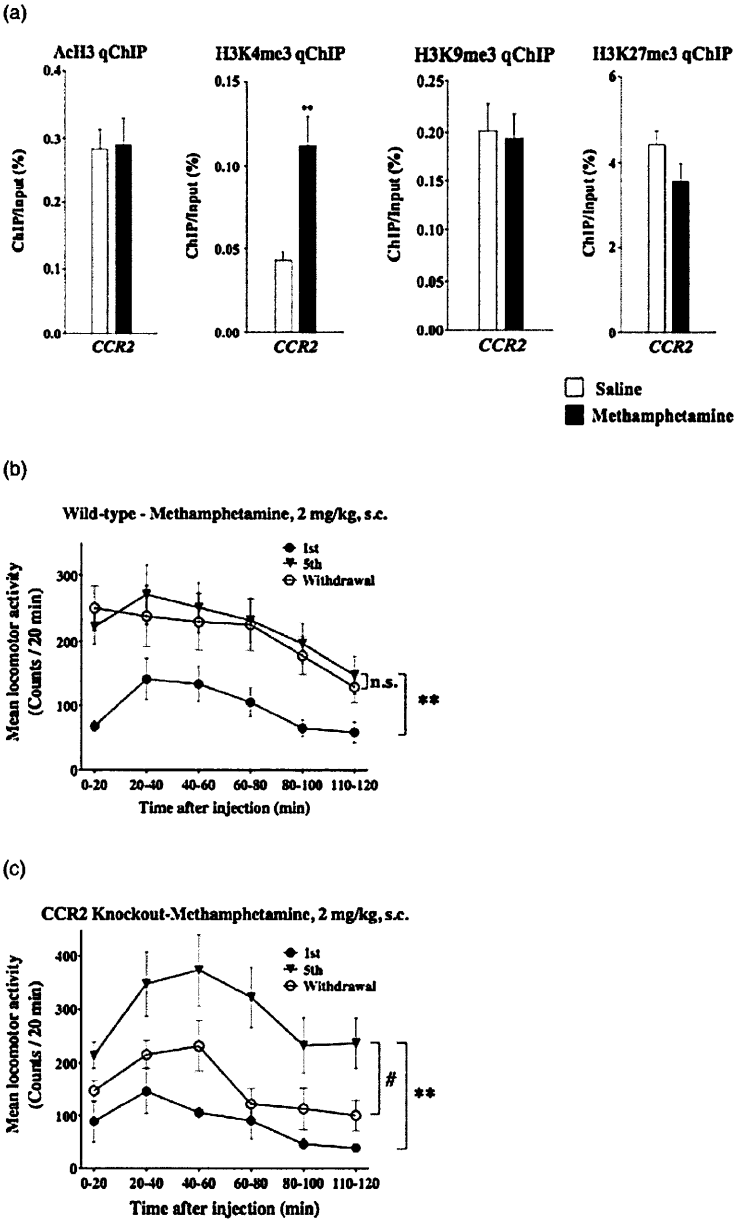

Figure 2 (a) qChIP analysis of acetylated histone H3 (AcH3), histone H3 trimethylated at lysine 4 (H3K4me3), lysine 9 (H3K9me3), and lysine 27 (H3K27me3) at CCR2 loci in the limbic forebrain of mice that had been intermittently treated with methamphetamine. Each column represents the mean ± SEM ($n = 4$ animals per group; three independent experiments). $^{**}P < 0.01$ versus saline-treated mice. (b) Change in locomotor activity (per 20 minutes time intervals) following intermittent administration of methamphetamine (2 mg/kg, s.c.) in wild-type mice (B-i) or CCR2 knockout mice (B-ii). Mice were treated intermittently with methamphetamine every 96 hours for five sessions. '1st' represents the 1st injection group, whereas 5th shows the 5th injection group. Mice described as 'withdrawal' were again administered methamphetamine after seven weeks of withdrawal. $^{**}P < 0.01$, 1st versus 5th, $\#P < 0.05$, 5th versus withdrawal (two-way ANOVA). n.s., not significant. Each point represents the mean ± SEM ($n = 4$–17 mice)

As shown in Fig. 1a, intermittent injection of methamphetamine produced a progressive increase in methamphetamine-induced locomotion, indicating the development of sensitization to methamphetamine (Fig. 1a, $F_{(4, 95)} = 4.940$, $P < 0.01$, first session versus fifth session).

As shown in Fig. 1b, a significant increase in mRNA of CCR2, but not of IL-1β, IL-4, IL-6, IL-10, TNFα, TGFβ1, TGFβ2, TGFβ3, MCP-1, RANTES, MCP-3, CXCL12 or CXCR4, was observed in the limbic forebrain, mainly including the nucleus accumbens, of the mice that had shown behavioral sensitization to methamphetamine (Fig. 1b, $P < 0.01$ versus the saline-treated mice). CCR2 is a seven-transmembrane-spanning Gαi protein-coupled receptor for a member of the C-C chemokine family, MCP-1, and is considered to regulate various brain disorders (Yong & Rivest 2009).

To gain further insight into these phenomena, we next studied histone modifications at the promoter regions of the CCR2 gene (Iida *et al.* 2008). A ChIP assay, where tissue is lightly fixed to crosslink DNA with histones and other DNA-binding proteins and then immunoprecipitated for a protein of interest, can be used to assess the extent to which a given gene is associated with these markers of activation or repression. In this study, we analyzed two active histone modifications [acetylation of

histone H3 and trimethylation of lysine 4 on histone H3 (H3K4)] and two repressive histone modifications [trimethylation of lysine 9 on histone H3 (H3K9) and trimethylation of lysine 27 on histone H3 (H3K27)] at the CCR2 gene promoter in the limbic forebrain of mice that had been intermittently treated with methamphetamine. As a result, intermittent treatment with methamphetamine caused a significant increase in the level of H3K4 trimethylation at the CCR2 promoter in the mouse limbic forebrain (Fig. 2a, $P<0.01$ versus the saline-treated mice; Figs S1 and S2). Methamphetamine did not produce other histone modifications at the CCR2 gene promoter (Fig. 2a). To the best of our knowledge, the present data are the first to indicate that intermittent treatment with methamphetamine induces a dramatic increase in the expression of the CCR2 gene along with epigenetic modifications in the nucleus accumbens.

To address the functional relevance of the increased CCR2 expression after the intermittent administration of methamphetamine, we next investigated whether the reduction of CCR2 expression could affect behavioral sensitization to methamphetamine using CCR2 knockout mice (Fig. S3). As shown in Fig. 2b, the fifth injection of methamphetamine produced a dramatic and significant increase in methamphetamine-induced hyperlocomotion compared with the first injection in both C57BL/6J (wild-type) and CCR2 gene knockout mice to the same degree (wild-type: first versus fifth, $F_{(1,\ 160)} = 12.39$, $P < 0.01$, CCR2 knockout: first versus fifth, $F_{(1,\ 30)} = 20.00$, $P < 0.01$), indicating that lack of the CCR2 gene had little or no effect on the development of sensitization to methamphetamine-induced hyperlocomotion. Intriguingly, the sensitization to methamphetamine was maintained even after seven weeks of withdrawal following intermittent administration of methamphetamine in the wild-type mice (fifth versus withdrawal, $F_{(1,\ 110)} = 0.05$, no significant). However, the methamphetamine-induced sensitization was almost reversed after seven weeks of withdrawal in CCR2 knockout mice (fifth versus withdrawal, $F_{(1,\ 30)} = 8.50$, $P < 0.05$, Fig. 2b). These results indicate that CCR2 is implicated in the maintenance of behavioral sensitization to methamphetamine.

In conclusion, the present study suggests that the intermittent administration of methamphetamine increases the mRNA level of CCR2 in association with epigenetic modification at its promoter in the limbic forebrain including the nucleus accumbens, and this may correlate with the maintenance of sensitization to methamphetamine-induced hyperlocomotion.

References

Iida S, Watanabe-Fukunaga R, Nagata S, Fukunaga R (2008) Essential role of C/EBPalpha in G-CSF-induced transcriptional activation and chromatin modification of myeloid-specific genes. Genes Cells 13:313–327.

Renthal W, Nestler EJ (2008) Epigenetic mechanisms in drug addiction. Trends Mol Med 14:341–350.

Robinson TE, Kolb B (1999) Alterations in the morphology of dendrites and dendritic spines in the nucleus accumbens and prefrontal cortex following repeated treatment with amphetamine or cocaine. Eur J Neurosci 11:1598–1604.

Sokolov BP, Polesskaya OO, Uhl GR (2003) Mouse brain gene expression changes after acute and chronic amphetamine. J Neurochem 84:244–252.

Ujike H, Takaki M, Kodama M, Kuroda S (2002) Gene expression related to synaptogenesis, neuritogenesis, and MAP kinase in behavioral sensitization to psychostimulants. Ann N Y Acad Sci 965:55–67.

Vanderschuren LJ, Kalivas PW (2000) Alterations in dopaminergic and glutamatergic transmission in the induction and expression of behavioral sensitization: a critical review of preclinical studies. Psychopharmacology 151:99–120.

Yong VW, Rivest S (2009) Taking advantage of the systemic immune system to cure brain diseases. Neuron 64:55–60.

SUPPORTING INFORMATION

Additional Supporting Information may be found in the online version of this article:

Figure S1 qChIP analysis of acetylation of histone H3 (AcH3), H3K4me3, H3K9me3, and H3K27me3 in the limbic forebrain of mice that had been intermittently treated with methamphetamine (2 mg/kg, s.c., 5 times). Tubulin was used as a control for AcH3 and H3K4me3. High levels of AcH3 and H3K4me3 at the TATA box binding protein (Tbp) gene, which is transcriptionally activated within neurons, H3K9 and K27 trimethylation at silenced genes marker major satellite DNA, which probably comprises the functional centromere, and Gbx2 promoter (a homeobox-containing family of DNA-binding transcription factors) are seen in the limbic forebrain of methamphetamine-treated mice. Each column represents the mean ± S.E.M. ($n = 4$ animals per group; three independent experiments)

Figure S2 Representative PCR product with 40 cycles for CCR2 DNA in the limbic forebrain of mice that have shown behavioral sensitization to methamphetamine (ME). The limbic forebrain sample was prepared 24 hours after the last injection of saline (SA) or ME

Figure S3 Analysis of CCR2 mRNA expression by RT-PCR in the mouse whole brain from wild-type (WT) and CCR2 knockout (KO) mice

Table S1 Comprehensive list of all primer sequences used.

Appendix S1 Supplemental methods

Please note: Wiley-Blackwell are not responsible for the content or functionality of any supporting materials supplied by the authors. Any queries (other than missing material) should be directed to the corresponding author for the article.

SYNAPSE 64:721–728 (2010)

Short Communication

Enhanced IL-1β Production in Response to the Activation of Hippocampal Glial Cells Impairs Neurogenesis in Aged Mice

NAOKO KUZUMAKI,[1] DAIGO IKEGAMI,[1] SATOSHI IMAI,[1] MICHIKO NARITA,[1] RIE TAMURA,[1] MARIE YAJIMA,[1] ATSUO SUZUKI,[1] KAZUHIKO MIYASHITA,[1] KEIICHI NIIKURA,[1] HIDEYUKI TAKESHIMA,[2] TAKAYUKI ANDO,[2] TOSHIKAZU USHIJIMA,[2] TSUTOMU SUZUKI,[1] AND MINORU NARITA[1]*

[1]*Department of Toxicology, Hoshi University School of Pharmacy and Pharmaceutical Sciences, 2-4-41 Ebara, Shinagawa-ku, Tokyo 142-8501, Japan*

[2]*Carcinogenesis Division, National Cancer Center Research Institute, 5-1-1 Tsukiji, Chuo-ku, Tokyo 104-0045, Japan*

[Correction to title made after initial online publication.]

KEY WORDS aging; hippocampus; astrocytes; microglia; IL-1β; neurogenesis

A variety of mechanisms that contribute to the accumulation of age-related damage and the resulting brain dysfunction have been identified. Recently, decreased neurogenesis in the hippocampus has been recognized as one of the mechanisms of age-related brain dysfunction. However, the molecular mechanism of decreased neurogenesis with aging is still unclear. In the present study, we investigated whether aging decreases neurogenesis accompanied by the activation of microglia and astrocytes, which increases the expression of IL-1β in the hippocampus, and whether in vitro treatment with IL-1β in neural stem cells directly impairs neurogenesis. Ionized calcium-binding adaptor molecule 1 (Iba1)-positive microglia and glial fibrillary acidic protein (GFAP)-positive astrocytes were increased in the dentate gyrus of the hippocampus of 28-month-old mice. Furthermore, the mRNA level of IL-1β was significantly increased without related histone modifications. Moreover, a significant increase in lysine 9 on histone H3 (H3K9) trimethylation at the promoter of NeuroD (a neural progenitor cell marker) was observed in the hippocampus of aged mice. In vitro treatment with IL-1β in neural stem cells prepared from whole brain of E14.5 mice significantly increased H3K9 trimethylation at the NeuroD promoter. These findings suggest that aging may decrease hippocampal neurogenesis via epigenetic modifications accompanied by the activation of microglia and astrocytes with the increased expression of IL-1β in the hippocampus. **Synapse 64:721–728, 2010.** ©2010 Wiley-Liss, Inc.

INTRODUCTION

The stability of life is constantly threatened by a wide range of internal and external stressors, and, under these circumstances, active maintenance is required to protect the integrity of the organism. It is widely accepted that aging is caused by the gradual, lifelong accumulation of a wide variety of molecular and cellular damage.

The hippocampus is one of the few areas of the rodent brain that continues to produce neurons postnatally (Eriksson et al., 1998). Neurogenesis in the dentate gyrus (DG) of the hippocampus occurs throughout the life of rodents. The aging hippocampus undergoes a variety of structural and functional alterations, which may be accompanied by decreased hippocampal neurogenesis (Kuhn et al., 1996).

Microglia are CNS-resident, macrophage-like cells of hematopoietic origin that play a role in the homeo-

This article was published online on 23 March 2010. An error was subsequently identified. This notice is included in the online and print versions to indicate that both have been corrected 24 May 2010.

*Correspondence to: Minoru Narita, Department of Toxicology, Hoshi University School of Pharmacy and Pharmaceutical Sciences, 2-4-41 Ebara, Shinagawa-ku, Tokyo, 142-8501, Japan. E-mail: narita@hoshi.ac.jp

Received 1 December 2009; Accepted 16 February 2010

DOI 10.1002/syn.20800

Published online 23 March 2010 in Wiley InterScience (www.interscience.wiley.com).

stasis of the healthy CNS and as immune surveillance cells in response to infection and injury. When neurons are injured as a result of aging or neurodegeneration, microglia become activated via the release of ATP, neurotransmitters, growth factors or cytokines, chemokines, ion changes in the local environment, or a loss of inhibitor molecules displayed by healthy neurons (Lucin and Wyss-Coray, 2009).

In there role as cells that provide multiple forms of support to the CNS, astrocytes are beginning to be appreciated as suppliers of critical survival and differentiation factors to neurons and other glial cells. Recent studies have suggested that astrocytes may express cytokines, chemokines, and growth factors as well as neurotransmitters throughout life, and not only in the developing fetus. Further studies on brain damage have suggested that, like microglia, astrocytes may be over-activated with aging (Labourdette and Eclancher, 2002).

Cytokines and chemokines are small, mostly secreted proteins that were originally characterized as immune modulators, but they have subsequently been found to mediate a diverse array of functions in glial cells that reside in the brain as well as peripheral glial cells and immunocells. Recently, it has been reported that excessive IL-1β contributes to the antineurogenic effect (Koo and Duman, 2008). Thus, in this study, we investigated whether aging increases IL-1β in the hippocampus associated with the activation of microglia and astrocytes, and whether in vitro treatment with IL-1β affects neural stem cell differentiation.

This study was conducted in accordance with the Guiding Principles for the Care and Use of Laboratory Animals, Hoshi University, as adopted by the Committee on Animal Research of Hoshi University, which is accredited by the Ministry of Education, Culture, Sports, Science and Technology of Japan. All efforts were made to minimize the number of animals used and their suffering.

Two- and from 24- to 28-month-old C57BL/6J mice (Jackson Laboratories, Bar Harbor, ME) were used in this study. Animals were kept in a room with an ambient temperature of 23 ± 1°C and a 12-h light/dark cycle (lights on 8:00 AM–8:00 PM). Food and water were available ad libitum. This study was approved by the Animal Research Committee of Hoshi University.

Mice were deeply anesthetized with isoflurane (3%) and perfusion-fixed with 4% paraformaldehyde (pH 7.4). The brain was then quickly removed and the hippocampus was rapidly dissected and postfixed in 4% paraformaldehyde for 2 h. The hippocampus was permeated with 20% sucrose for 1 day and 30% sucrose for 2 days, and then frozen in an embedding compound (Sakura Finetechnical, Tokyo, Japan). All samples were stored at −30°C until use. The sections were cut transversely at a thickness of 8 μm on a cryostat (Leica CM1510, Leica Microsystems, Heidelberg, Germany). The hippocampus sections were blocked in 10% normal goat serum in 0.01M phosphate-buffered saline (PBS) for 1 h at room temperature. Each primary antibody was diluted in 0.01M PBS containing 10% normal goat serum glial fibrillary acidic protein (GFAP), (1:20 Nichirei, Tokyo, Japan) or ionized calcium-binding adaptor molecule 1, (Iba1) (1:130 Wako Pure Chemicals, Osaka, Japan), and incubated for 2 days overnight at 4°C. The samples were then rinsed and incubated with the appropriate secondary antibody conjugated with Alexa 488 (Invitrogen, Carlsbad, CA) for 2 h at room temperature. The slides were then coverslipped with Perma-Fluor Aqueous mounting medium (Immunon, Pittsburgh, PA). Fluorescence of immunolabeling was detected using a light microscope (Olympus AX-70; Olympus, CO, Tokyo, Japan) and a Radiance 2000 laser-scanning microscope (BioRad, Richmond, CA), and photographed with a digital camera (Polaroid PDMCII/OL; Olympus, CO, Tokyo, Japan).

Two- and from 24- to 28-month-old mice (Jackson Laboratories, Bar Harbor, ME) were used for Western blotting. Each hippocampus was individually homogenized in ice-cold buffer A containing 20 mM Tris-HCl (pH 7.5), 2 mM EDTA, 0.5 mM EGTA, 1 mM phenylmethylsulfonyl fluoride, 25 μg of leupeptin per ml, 0.1 mg of aprotinin per mL, and 0.32M sucrose. The homogenate was centrifuged at 1000 × *g* for 10 min and the supernatant was ultracentrifuged at 100,000 × *g* for 30 min at 4°C. The pellets were washed with buffer B (buffer A without sucrose) and then ultracentrifuged at 100,000 × *g* for 30 min. The final pellets were retained as the membranous fraction for Western blotting at −80°C until the assay. Protein concentration in the samples was assayed by the method of Bradford et al. (Bradford, 1976). An aliquot of tissue sample was diluted with an equal volume of 2× electrophoresis sample buffer (Protein Gel Loading Dye-2×; Amresco, Solon, OH) containing 2% sodium dodecyl sulfate (SDS) and 10% glycerol with 0.2M dithiothreitol. Proteins (10–20 μg/lane) were separated by size on 4–20% SDS-polyacrylamide gradient gel using the buffer system, and then transferred to nitrocellulose membranes in Tris-glycine buffer containing 25 mM Tris and 192 mM glycine. For immunoblot detection, the membranes were blocked in Tris-buffered saline (TBS) containing 1% nonfat dried milk with 0.1% Tween 20 (Bio-Rad Laboratories, Hercules, CA) for 1 h at room temperature with agitation. The membrane was incubated with primary antibody diluted in TBS containing 1% nonfat milk with 0.1% Tween 20 [1:1000 GFAP (Nichirei, Tokyo, Japan), 1:1000 Iba1 (Wako Pure Chemicals, Osaka, Japan)] overnight at 4°C. The membrane was washed in TBS containing 0.05% Tween 20 (TTBS), and then incubated for 2 h at room temperature with

horseradish peroxidase-conjugated antirabbit IgG (Southern Biotechnology Associates, Birmingham, AL) diluted 1:10,000 in TBS containing 1% nonfat dried milk with 0.1% Tween 20. To control for validation in loading, we assayed the expression of a housekeeping gene by Western blot analysis. After incubation with primary and secondary antibodies, the membrane was then re-probed with mouse anti-GAPDH polyclonal antibody [GFAP: 1:200,000 in TBS containing 1% nonfat milk with 0.1% Tween 20, Iba1: 1:50,000 in 5% nonfat milk (Chemicon International, Temecula, CA)] for 1 h, and then incubated with anti-mouse secondary antibody conjugated with horseradish peroxidase (1:10,000) for 2 h at room temperature. The antigen–antibody peroxidase complex was finally detected by enhanced chemiluminescence (Pierce, Rockford, IL) according to the manufacturer's instructions and visualized by exposure to Amersham Hyperfilm (Amersham Life Sciences, Arlington Heights, IL).

Total RNA in the hippocampus of aged mice was extracted using the SV Total RNA Isolation system (Promega, Madison, WI) following the manufacturer's instructions. Purified total RNA was quantified spectrophotometrically at A_{260}. To prepare first-strand cDNA, 1 μg of RNA was incubated in 100 μl of buffer containing 10 mM dithiothreitol, 2.5 mM $MgCl_2$, dNTP mixture, 50 U of reverse transcriptase II (Invitrogen, Carlsbad, CA) and 0.1 mM oligo-$dT_{12\text{-}18}$ (Invitrogen, Carlsbad, CA). Each gene was amplified in 50 μl of PCR solution containing 0.8 mM $MgCl_2$, dNTP mixture, and DNA polymerase with synthesized primers: IL-1β, F; 5′-CAC TAG GTT TGC CGA GTA GAT CTC-3′, R; 5′-GTG CTG CCT AAT GTC CCC TTG AAT C-3′, NeuroD, F; 5′-GCA TGC ACG GGC TGA ACG C-3′, R; 5′-GGG ATG CAC CGG GAA GGA AG-3′, GAPDH, F; 5′-CCC ACG GCA AGT TCA ACG G-3′, R; 5′-CTT TCC AGA GGG GCC ATC CA-3′. Samples were heated to 94°C for 30 s, 55°C for 1 min, and 72°C for 1 min. The final incubation was at 72°C for 7 min. The mixture was run on 2% agarose gel electrophoresis with the indicated markers and primers for the internal standard glyceraldehyde-3-phosphate dehydrogenase. The agarose gel was stained with ethidium bromide and photographed with UV transillumination. The intensity of the bands was analyzed and semiquantified by computer-assisted densitometry using ImageJ software.

Fast SYBR Green Master Mix (Applied Biosystems, Foster City, CA) was used as the basis for the reaction mixture in the real-time PCR assay. Each gene prepared by the above procedure was amplified in 20 ml of a PCR solution containing 10 ml of the Fast SYBR Green Master Mix with synthesized primers: NeuroD, F; 5′-GCA TGC ACG GGC TGA ACG C-3′, R; 5′-GGG ATG CAC CGG GAA GGA AG-3′, β-actin, F; 5′-CAG CTT CTT TGC AGC TCC TT-3′, R; 5′-TCA CCC ACA TAG GAG TCC TT-3′. In addition to each sample, each test run included a no-target control that contained reaction mixture and PCR-grade water. PCR with a StepOnePlus™ (Applied Biosystems, CA) was performed with the following cycling conditions: 95°C for 20 s, followed by 45 cycles of 95°C for 3 s and 60°C for 30 s. Fluorescence detection was conducted after each extension step.

A ChIP assay was performed as described previously (Tsankova et al., 2004; Takeshima et al., 2009) with minor modifications. Briefly, mouse hippocampus tissue was dissected as described above and cross-linked, and the tissue was then lysed. Fifteen μg of soluble chromatin was incubated with 2 μg of specific antibodies; against acetylated histone H3 (Millipore, Billerica, MA); H3K4 trimethylation (Wako Pure Chemicals, Osaka, Japan); H3K9 trimethylation (Millipore, Billerica, MA); or H3K27 trimethylation (Millipore, Billerica, MA), overnight at 4°C. The immuno-complex was collected by Dynabeads Protein A (Invitrogen, Carlsbad, CA), and DNA was recovered with RNaseA treatment, Proteinase K treatment and isopropanol precipitation. Immunoprecipitated DNA was dissolved in 50 μl of 1× TE and 1 μl was used for quantitative PCR. Quantitative PCR was performed as described previously (Nakajima et al., 2009). IL-1β, F; 5′-TCC ACC ACG ATG ACA CAC TT-3′, R; 5′-GGG AGA AGC TTG ATG GGA AT-3′, NeuroD, F; 5′-GCA TGC ACG GGC TGA ACG C-3′, R; 5′-GGG ATG CAC CGG GAA GGA AG-3′.

Pregnant C57BL/6J mice were used to prepare NSCs. NSCs were obtained from whole brain of E14.5 mice and cultured. Briefly, the brain were triturated in serum-free medium: Dulbecco's modified Eagle's medium with 4500 mg/L glucose, 5 μg/ml insulin, 10 ng/ml EGF, 50 μg/ml transferrin, 10 ng/ml biotin, and 30 nM Na_2SeO_3. EGF (10 ng/ml) was used to keep the cultures proliferating. For differentiation experiments, ~10 neurospheres of the same size were isolated with a pipette and deposited on 10 μg/ml laminin-coated glass slides with 400 μl of serum-free medium with 10 ng/ml EGF. The NSCs were incubated overnight in medium containing EGF, which was then replaced by medium without EGF but containing IL-1β (10, 100 ng/ml) for 7 days. Differentiated neurospheres were fixed with 4% paraformaldehyde for 20 min at room temperature and processed for immunocytochemistry (ICC). The samples were rinsed with PBS twice and pretreated with PBS containing 0.3% Triton-X100 for 5 min at room temperature for ICC. After blocking in blocking buffer (PBS containing 5% FBS and 0.3% TritonX) for 1 h at room temperature, the samples were incubated at 4°C overnight with the following antibodies: antiβIII-tubulin (mouse IgG, 1:1000, Sigma-Aldrich, St. Louis, MO, T8660) After three washes with PBS, the samples were incubated for 1 h at room temperature with secondary antibodies conjugated with Alexa488 (Invi-

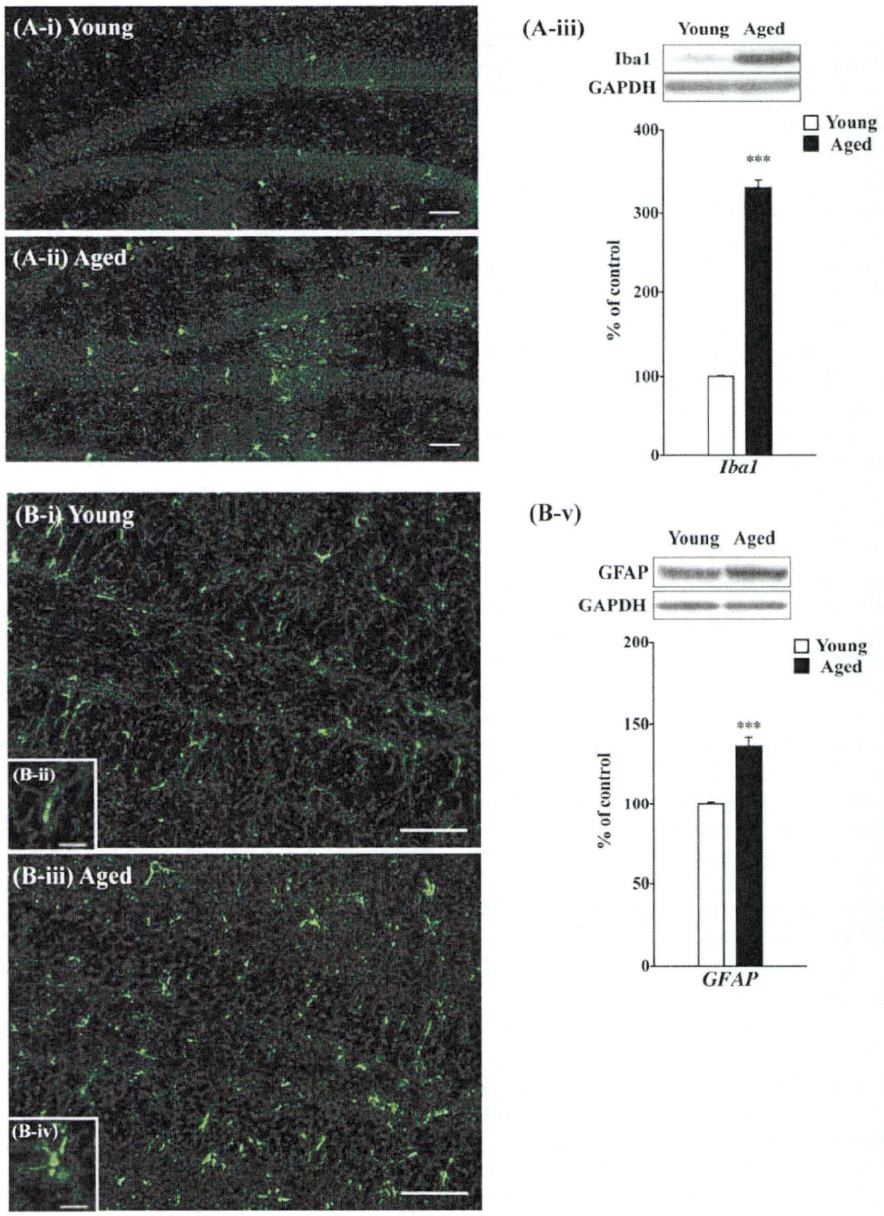

Fig. 1. **A**: Immunofluorescent staining for ionized calcium-binding adaptor molecule 1 (Iba1) in the dentate gyrus (DG) in young and aged mice. Iba1-like IR in the DG of aged mice (A-ii) was increased compared to that in young mice (A-i). Scale bar: 50 μm. (A-iii) *Upper*: Representative Western blot of Iba1. *Lower*: Changes in IR for Iba1 in the cytosolic fraction of hippocampus obtained from aged mice. Each column represents the mean ± SEM of six samples (***$P < 0.001$ vs. young group). **B**: Immunofluorescent staining for glial fibrillary acidic protein (GFAP) in the DG in young and aged mice. GFAP-like IR in the DG of aged mice (B-iii, B-iv: high magnification) was increased compared to that in young mice (B-i, B-ii: high magnification). Scale bar: 50 μm (B-i,-iii). Scale bar: 10 μm (B-ii, iv). (B-v) *Upper*: Representative Western blot of GFAP. *Lower*: Changes in IR for GFAP in the membranous fraction of hippocampus obtained from aged mice. Each column represents the mean ± SEM of 6 samples (***$P < 0.001$ vs. young group).

trogen, Carlsbad, CA) After being washed with PBS, the samples were mounted on slides and examined with microscope with a 10× objective lens (IX 71, Olympus, CO, Tokyo, Japan) and photographed with a digital camera (VB-6000, Keyence, CO, Osaka, Japan).

NSCs (5×10^5 cells per well) were treated with IL-1β (10 ng/ml, 100 ng/ml) for 8 h in 96-well plates. Afterward, the numbers of viable cells in culture were determined using the CellTiter-Glo Luminescent Cell Viability Assay kit (Promega, Madison, WI), which

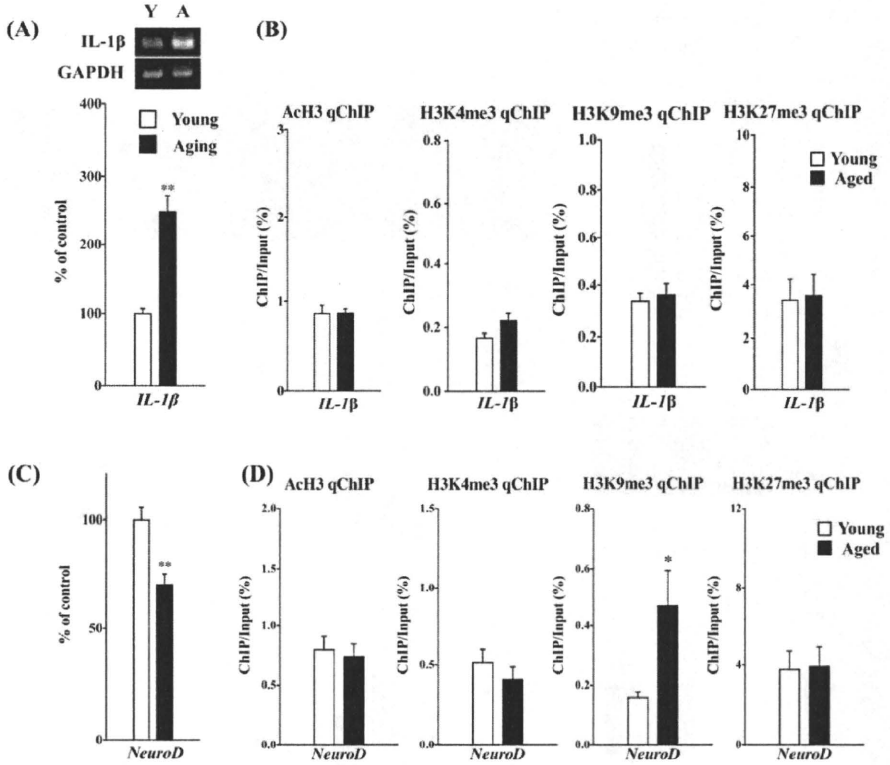

Fig. 2. **A**: *Upper*: Representative RT-PCR for IL-1β mRNA in the hippocampus obtained from young and aged mice. *Lower*: The intensity of the bands was semi-quantified using NIH Image software. The value for mRNA was normalized by that for the internal standard glyceraldehyde-3-phosphate dehydrogenase (GAPDH) mRNA. The value for aged mice is expressed as a percentage of the increase in young mice. Each column represents the mean ± SEM of three samples. (**$P < 0.01$ vs. young group). **B**: qChIP analysis of acetylated histone 3 (AcH3), histone 3 trimethylated at lysine 4 (H3K4me3), lysine 9 (H3K9me3), and lysine 27 (H3K27me3) at IL-1β loci in the hippocampus obtained from young and aged mice. Each column represents the mean ± SEM of three samples. **C**: Quantitative analysis of NeuroD mRNA in the hippocampus obtained from young and aged mice. Each column represents the mean ± SEM of 3 samples. (**$P < 0.01$ vs. the young group). **D**: qChIP analysis of AcH3, H3K4me3, H3K9me3 and H3K27me3 at NeuroD loci in the hippocampus obtained from young and aged mice. Each column represents the mean ± SEM of six samples (*$P < 0.05$ vs. young group).

evaluates the presence of ATP, an indicator of metabolically active cells, according to the manufacturer's instructions. All experiments were performed in triplicate wells.

The data are expressed as the mean ± SEM The statistical significance of differences between groups was assessed with Student's *t*-test (comparison of two groups) or an analysis of variance (ANOVA) followed by the Bonferroni test (comparison among multiple groups). A level of probability of 0.05 or less was considered significant.

To investigate a possible change in glial cell activity in the hippocampus of aged mice, immunohistochemical studies were performed. As shown in Figure 1A, the immunoreactivity (IR) of the specific microglial marker Iba1 was prominently observed in the DG of young mice (Fig. 1A-i). In the DG of aged mice, Iba1-IR was dramatically increased compared with that in young mice (Fig. 1A-ii). Western blots showed that the levels of Iba1 were significantly increased in the hippocampus of aged mice compared with those in young mice ($P < 0.001$; Fig. 1A-iii). Astrocytes in the DG of the hippocampus were stained with GFAP antibody. These astrocytes were sparsely distributed in young mice (Fig. 1B-i). In the DG of aged mice, IR for GFAP was increased compared with that in young mice (Fig. 1B-iii). Each individual astrocyte labeled by GFAP was hypertrophied with an enlarged cell body (Fig. 1B-ii and iv). Western blots showed that the level of GFAP was significantly increased in the hippocampus of aged mice compared with that in young mice ($P < 0.001$; Fig. 1B-v).

We next investigated the changes in the mRNA expression of IL-1β in the mouse hippocampus of young and aged mice. The mRNA expression of IL-1β was significantly increased in the hippocampus of aged mice compared with that in young mice ($P < 0.01$; Fig. 2A). To gain further insight into these phenomena, we next studied the histone modifications at the promoter regions of the IL-1β gene (Fig. 2B). As a